OPEN

Exploring 3D Printed Implants With Anti-Dropout Function to Overcome Time Constraints in Acute Orbital Fractures for Patient-Specific Implants

Dong Ha Park, MD, Jun Suk Lee, MD, Yeon Kyo Jung, MD, and Hyoseob Lim, MD, PhD

Abstract: Orbital wall reconstruction and implant insertion are crucial procedures for temporarily replacing the orbital walls in cases of significant fractures. Traditional methods using planar orbital implants have faced challenges owing to their flat shape, which increases the risk of dislocation from improper cuts and necessitates the use of screws in the orbital rim. This study aims to improve outcomes by employing customized 3-dimensional implants, thereby reducing complications and risk of dislocation resulting from external shock or implant weight postinsertion. This prospective study included 12 Korean individuals diagnosed with facial fractures (orbital wall injuries). Surgeries were performed on 12 patients, and follow-up CT scans were conducted on 10 of them. Therefore, the authors could only address the results for the 10 patients. The authors used bioactive glass ceramics and medical-grade poly-e-caprolactone to 3D print personalized implants, completing the manufacturing process in an average of 4.6 days. Computed tomography scans guided measurements of orbital volumes and exophthalmos. After surgery, we found that the difference values for bone orbital volumes (< 0.1 mL) and exophthalmos (< 1 mm except one) decreased compared with presurgery values. Independent *t* tests and Pearson correlation analysis revealed no significant changes between normal and affected sides in both phases. However, R-values increased in the postsurgery phase. Patients monitored postsurgery at 2 weeks, 3 months, and 6 months showed no complications. The 3D-printed patient-specific implants, customized to individual fracture shapes and featuring distinct implants and locking parts with notches, effectively restore bony orbital volumes and reduce exophthalmos. They have been proven feasible and applicable for reconstructing acute orbital wall fractures.

Key Words: BGS-7 (CaOSiO2-P2O5-B2O3 bioactive glass-ceramics), computer-aided design, enophthalmos, mirroring, PCL (Poly-e-caprolactone), orbital fractures, orbital implants, Patient-specific modeling

(*J Craniofac Surg* 2024;35: 2264–2268)

Among the most common fractures of the facial skeleton are those of the orbital floor and/or medial orbital wall. These fractures can lead to potentially serious functional and esthetic complications, such as swelling, hematoma, bulbar deformity, eyeball motility disorders, diplopia, globe malposition.[1–3]

Currently, orbital wall reconstruction is conducted when the extent and severity of the fracture are significant. In addition, an orbital implant that replaces the broken bone is inserted, and the orbital soft tissue that herniated through the fracture site is repaired. Depending on the type of implant used, it temporarily replaces the orbital wall until the broken orbital wall is repaired or permanently replaces the fractured orbital bones.

Traditionally, surgeons have relied on commercially available planar orbital implants for reconstruction. However, this method involves manually cutting and shaping the implant to fit the fracture site, relying solely on the surgeon's visual assessment. Unfortunately, the inherent flatness of these implants often poses challenges in accurately replicating the 3-dimensional shape and curvature of the orbital wall. As a result, the accuracy of manually crafted implants depends heavily on the surgeon's experience and skill. This can lead to multiple attempts at implant insertion during surgery, which may cause damage to orbital soft tissues and prolong operation times. In addition, mismatched implants may result in dislocation and potential complications such as diplopia or asymmetric ocular protrusion. To mitigate these risks, some surgeons have resorted to additional measures such as screw fixation to the inferior orbital rim. However, using ill-fitting and improperly fixed implants can further exacerbate risks in certain cases.

Patient-specific implants (PSIs) present a promising solution in response to these challenges. However, the conventional manu-

From the Department of Plastic and Reconstructive Surgery, Ajou University School of Medicine, Suwon, Gyeonggi-do, Republic of Korea.

Received June 30, 2024.
Accepted for publication August 22, 2024.

Address correspondence and reprint requests to Hyoseob Lim, MD, PhD, Ajou University School of Medicine, Suwon, Gyeonggi-do, Republic of Korea; E-mail: hyoseob.lim@gmail.com

This study was approved by the appropriate Institutional Review Board of Ajou Medical Center (AJOUIRB-DEV-2022-219) and adhered to the Declaration of Helsinki on Medical Protocol and Ethics. Before inclusion in the study, written informed consent was obtained from all participants.

Supported by the Korea Medical Device Development Fund grant funded by the Korean government (Ministry of Science and ICT, Ministry of Trade, Industry and Energy, Ministry of Health & Welfare, and Ministry of Food and Drug Safety) (Project Number: RS-2022-00140399).

Supplemental Digital Content is available for this article. Direct URL citations are provided in the HTML and PDF versions of this article on the journal's website, www.jcraniofacialsurgery.com.

The authors report noconflicts of interest.

ISSN: 1049-2275
DOI: 10.1097/SCS.0000000000010647

facturing process, particularly in acute fracture cases, encounters hurdles due to prolonged production timelines. To overcome this limitation, using 3D printing technology has emerged as a potential solution. In addition, the flexibility offered by 3D printing technology enables easy modifications of designs.

Taking into account the aforementioned points, we have developed novel implants with distinct features to protect the commonly injured inferior oblique muscle during surgery for inferomedial orbital fractures. These implants, designed in 2 separate pieces with locking parts, are inserted through individual incisions for the medial wall and the floor and joined together inside the orbital cavity as a single unit, preventing postinsertion dislocation caused by external forces or implant weight. This innovative design ensures effective restoration of the original shape, even in patients with collapsed orbital struts.

This paper delves into the feasibility and advantages of utilizing 3D printing to overcome time constraints associated with acute orbital fractures, enabling the timely application of PSIs. The aim is to reduce complications and improve patient outcomes by utilizing 3-dimensional printed implants tailored to each patient's unique fracture shape.

METHODS

Study Participants

We prospectively examined 12 Korean individuals diagnosed with medial orbital wall fracture, orbital floor fracture, or inferomedial orbital wall fracture (excluding blow-in fracture) between February and May 2023, who had bone defects measuring 2 cm^2 or larger, as indicated by computed tomography (CT) scans, suggesting anticipated enophthalmos. The characteristics of the patients were assessed, and the duration for implant fabrication, as well as the time elapsed from the patient's injury to the surgery, was determined. This study was approved by the Ajou Medical Center's Institutional Review Board (AJOUIRB-DEV-2022-219) in compliance with the Declaration of Helsinki on Medical Protocol and Ethics. Before inclusion in the study, written informed consent was obtained from all participants.

Data Acquisition and Image Processing

CT images were obtained using 64-section and 16-section multidetector CT scanners. Settings included a section thickness of 1 mm, maximum scanning time of 10 seconds, matrix size of 300×2000, voltage of 120 kV, and current of 250 mA. Images were viewed using PiView STAR and converted to DICOM format. AVIEW Research software was used for 3D reformation and parameter evaluation.

Material Preparation

CaO-SiO2-P2O5-B2O3 Bioactive glass ceramics (BGS-7, CGBIO, South Korea) and medical-grade poly-e-caprolactone (PCL, #PURASORB PC12, CorbionPurac, the Netherlands) were used. The material was approved for clinical investigation by the Ministry of Food and Drug Safety of Korea (ESMPB15). PCL and BGS-7 were combined in an 8:2 ratio, physically mixed, and freeze-milled. The average particle size of BGS-7 after freeze-milling was measured at 2.1 ± 0.2 μm.

Modeling

3D modeling software (Geomagic Freeform Plus; 3D Systems, Washington, DC) was used to design the implant. A single implant was designed for medial orbital wall orbital floor fractures. In cases of inferomedial fractures, the implant was divided into 2 sections to improve accessibility and preserve the inferior oblique muscle. The implants were designed to be slightly larger than the bone defect. Throughout the design process, the surgeon made adjustments to the shape, size, and curvature and incorporated "notches" on the surface opposite the eyeball of the implant to bolster its strength and prevent dislocation. The 2 implants featured "locking parts" resembling door hinges at the connecting points (Figs. 1 and 2). In cases where the orbital strut collapsed, additional "supporting notches" were incorporated into the locking parts to support the implant over the collapsed bone. The surface of the implants was smoothed, and multiple holes were designed to allow for the drainage of hematoma.

Manufacturing

The PCL/BGS-7 combination was heated to 90 °C for 15 to 30 minutes in a heating barrel and then linked to a LUCA system 3D printer (LUCA 300, CGBIO, Seongnam, South Korea). Using computer-aided manufacturing software, a deposition system was utilized to 3D print the mixture. The printing process involved layer-by-layer deposition of the melted liquid through a 400 μm-diameter nozzle. The melt was extruded by applying pneumatic pressure between 550 and 650 kPa. The resulting product is suitable for sterilization by Greenpia Technology Inc.'s continuous-type gamma irradiator, accredited by DNV Notified Body (ISO 9001:2015, EN/ISO 13485:2016 including ISO 11137), and registered by the US FDA (Device listing for an implant, etc.).[4]

A 3-dimensional image of the skull was created by converting the patient's CT scans depicting orbital wall fractures. The implant's form was then designed using this data. The implant (Easymade, CGBio, Seoul, Korea) utilizes fused deposition modeling in 3D printing and comprises PCL and BGS-7. A total of 12 PSIs were produced and subsequently applied to 12 patients.

Patient Follow-Up and Measurements of Bony Orbital Volumes and Degree of Exophthalmos

Patients were monitored at 2 weeks, 3 months, and 6 months postoperatively to assess for complications. CT scans were conducted immediately after the operation and repeated 6 months postoperatively. Since only 10 patients underwent CT scans at 6 months postsurgery, three-dimensional reformations of these 10 bony orbital cavities were generated using AVIEW Research software (Coreline Soft Inc., Seoul, South Korea). Facial bone landmarks, including the frontal zygoma process for the lateral orbital rim, anterior lacrimal crest for the inferomedial orbital rim, nasal process of the frontal bone for the superomedial orbital rim, and superior/inferior orbital rim, were

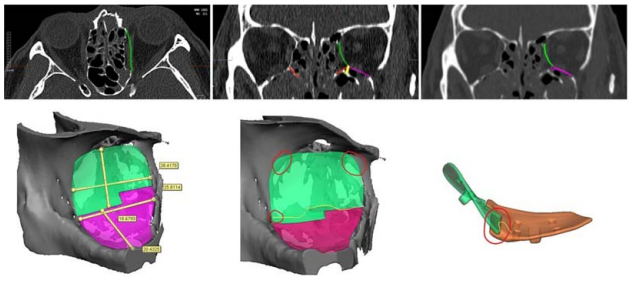

FIGURE 1. Communication for implant design. During the implant design, surgeons provide necessary implant requirements based on CT information they capture. Subsequently, implant manufacturers implement the implant shape through 3D rendering. Surgeons then provide detailed conditions, and the manufacturer communicates by reflecting these conditions in the design.

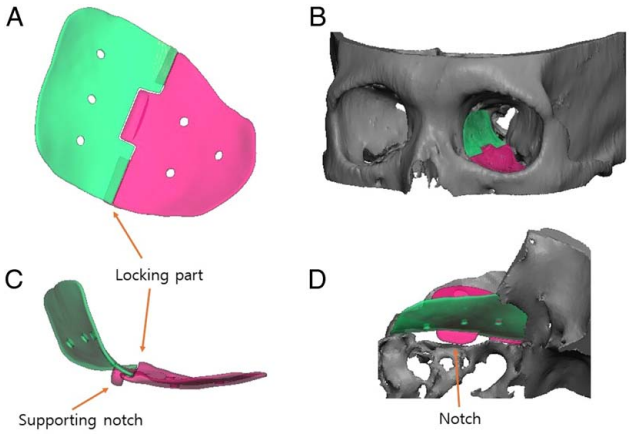

FIGURE 2. Specific implant design. Implants are manufactured in 2 pieces, one for the medial wall and one for the floor (inferior) purposes. (A, B) These 2 pieces are connected at the "locking part," like interlocking puzzle pieces, ensuring they do not overlap while forming a single unit. (A, C) A notch smaller than the bone defect size is created superiorly for fusion to facilitate proper implant positioning while preventing displacement. (D) A "supporting notch" is added to maintain three-dimensional positioning support in collapsed orbital struts. (C)

marked in a region of interest (ROI). Measurements, averaged from 2 independent evaluators specializing in plastic surgery and radiology, were conducted, excluding the optic canal or nasolacrimal duct. ROI selection on each CT slice enabled the computation of bone orbital volumes.[5–7]

The following formula was employed for volume calculation:

$$\text{volume} = (\text{numberofvoxels}) \times (\text{sizeofonevoxel}),$$

where the size of one pixel is represented by "pixel spacing × (mm) × pixel spacing Y (mm) × slice interval (mm)."

To assess the degree of exophthalmos, a horizontal line connecting the lateral orbital rim on both sides was drawn in the axial view cut of the CT scan where the cornea protrudes the most. Subsequently, a line perpendicular to the horizontal line and the cornea's maximum protrusion point were drawn to measure the vertical distance.[8]

Statistical Analysis

Independent *t* test and Pearson correlation coefficient test were used to analyze "differences in the bony orbital volumes and the degree of exophthalmos between the normal and affected side." Statistical significance was set at $P < 0.05$. All statistical analyses were performed using SPSS 29.0.1.0 software (IBM Corporation, Armonk, NY).

To enhance the precision of the bone orbital volume and degree of exophthalmos measuring technique, we also examined the interclass correlation coefficient (ICC). The continuous, normally distributed variables measured by raters 1 and 2 met the ICC's fundamental presumptions.

RESULTS

Among the 12 surgical patients, 10 completed all follow-up observations. The average time taken from obtaining CT data, designing, manufacturing, and sterilizing the implants was 4.6 days (range: 4–6 d), while the average time from injury to surgery was 11.8 days (range: 8–15 d) among these 12 patients (Supplemental Table 1, Supplemental Digital Content 1, http://links.lww.com/SCS/G732).

Preoperative and postoperative (at the 6-month follow-up) bony orbital volumes, degree of exophthalmos, and difference values (DVs) were measured among 10 patients who underwent follow-up CT. Compared with the preoperative phase, the difference values (difference between normal and affected side) for bony orbital volumes and the degree of exophthalmos decreased postoperatively (Supplemental Table 2, Supplemental Digital Content 1, http://links.lww.com/SCS/G732). After surgery, the DVs for volume (DVVs) were recorded to be 0.1 mL or less in all cases. In addition, the DVs in the degree of exophthalmos (DVXs) were recorded to be 2 mm or less in all cases and 1 mm or less in all cases except one.

Upon reviewing the postsurgery coronal CT scans of patients with inferomedial orbital wall fractures who underwent surgery with 3D-printed patient-specific implants, it is evident that the implants are appropriately positioned (Fig. 3).

We employed an independent *t* test and Pearson correlation analysis to examine bone orbital volumes and the degree of exophthalmos on affected and normal sides. There were no statistically significant changes between normal and affected sides in both preoperative and postoperative phases. However, in contrast to the preoperative phase, R-values increased throughout the postoperative phase (Supplemental Table 3, Supplemental Digital Content 1, http://links.lww.com/SCS/G732).

The inter-rater reliability evaluations for raters 1 and 2's measurements of orbital volumes and exophthalmos showed

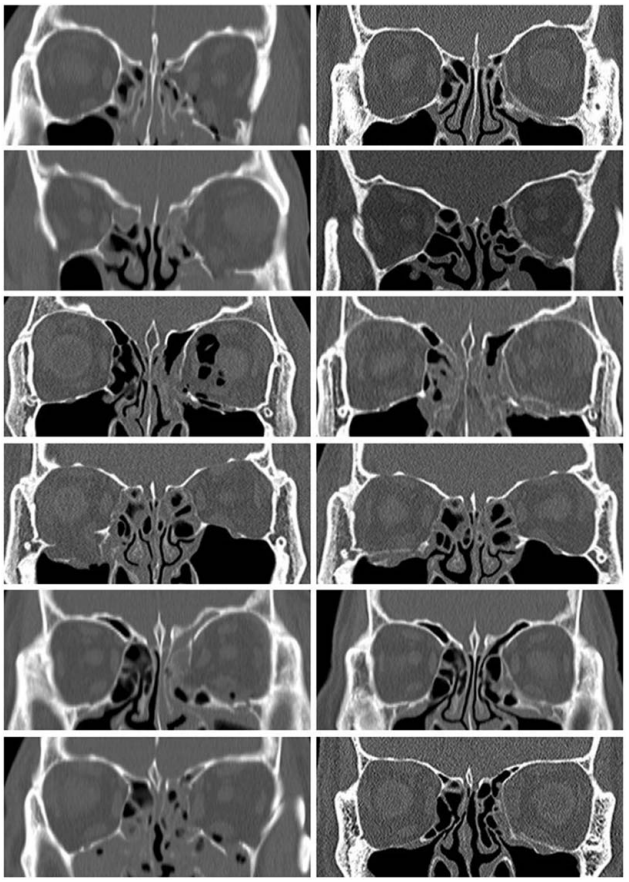

FIGURE 3. Preoperative and postoperative computed tomography (CT). After examining the coronal CT scans obtained after surgery from patients with inferomedial orbital wall fractures who received 3D-printed implants customized for them.

ICCs (2,1) of 0.995 ($P < 0.001$) and 0.994 ($P < 0.001$), respectively, indicating a measurement consistency of 99.5% and 99.4%, respectively (Supplemental Table 4, Supplemental Digital Content 1, http://links.lww.com/SCS/G732). Furthermore, patients who were followed up immediately after the operation, at 2 weeks, 3 months, and 6 months, did not show any complications. Two patients who were lost to follow-up were contacted by phone at 6 months postoperatively, and both reported no significant complications.

DISCUSSION

Despite meticulous preoperative planning and careful design in the operating room, we frequently face challenges in achieving satisfactory results during surgery for orbital wall fractures. This is particularly pronounced in cases of inferomedial wall fractures, where the variability in shapes among patients, and even within the same patient, depending on the location, as well as the diverse changes in curvature, pose significant challenges. When surrounding fractures are severe, the clarity of information regarding the normal structure and its positioning diminishes. In addition, in cases where the orbital strut collapses, there is a lack of support available. Furthermore, efforts to preserve the inferior oblique muscle can hinder the insertion of large, structurally strong implants into the fractured area.

Recent advancements in medicine have enabled the use of PSIs, providing significant assistance in orbital wall fracture surgery, especially with the incorporation of navigation during surgery.[9] However, the prolonged time required for manufacturing PSIs has limited their practical application mainly to patients undergoing tumor resection or those with post-traumatic orbital deformities, wherein ample time has elapsed since the injury.

With the recent strides in 3D printing and 3D simulation programs, the production time for PSIs has been notably shortened. Although concerns persist regarding the stability of materials used in 3D printing, the advent of this technology has unlocked avenues for deploying PSIs, even in cases of acute fractures.

This study aimed to evaluate the feasibility and stability of newly designed 3D-printed PSIs. Each novel implant is divided into 2 parts to mitigate the risk of injury to the inferior oblique muscle. After effortless insertion into the orbit, the parts seamlessly merge into a unified piece, allowing for the maintenance of the desired curvature, accurate placement in the desired position, and prevention of displacement due to gravity or external forces. These implants incorporate specialized design elements such as "notch," "locking part," and "supporting notch."

Reconstructing orbital wall fractures has involved using various materials, including nonmetallic and metallic options, such as titanium. We prioritize materials that are thin yet sturdy for implants. However, they should not be too strong to threaten the orbit if subjected to strong external forces postrecovery.[10] Therefore, although metallic materials can be easily shaped, they have been excluded. While the utilization of 3D-printed PSIs, incorporating materials like polymethylmethacrylate (PMMA), polyetherketone (PEEK), and PCL, has found applications across various domains, the optimal materials for 3D-printed PSIs in craniomaxillofacial surgery, including orbital wall reconstruction, have yet to be fully realized.[11–16]

PCL (#PURASORB PC12, CorbionPurac, the Netherlands), a flexible and nontoxic material, is cost-effective. However, it lacks strength and durability, exhibits hydrophobic properties, and poor cell adhesion. BGS-7 (CGBIO, South Korea) is minimally toxic to humans, stimulate osteoblastic differentiation, structurally resemble human bone, and form a robust physical link with the bone. Despite exhibiting some brittleness, similar to other ceramics, combining PCL with BGS-7 helps overcome these drawbacks. The initial preservation of the bone's 3-dimensional shape and subsequent replacement with autologous tissue are crucial characteristics of materials employed for facial bone reconstruction. Some researchers have explored using stem cells to stimulate tissue integration during surgery.[17–19] Considering this, we assessed the stability and usefulness of a scaffold made from a combination of PCL and BGS-7 and its applications in PSIs.[20,21]

The challenge of applying PSIs in acute trauma cases stems from the prolonged duration between production and surgery. However, through 3D printing, we achieved an average production time of 4.6 days, ultimately reducing the time from trauma to surgery to ~2 weeks (11.3 d).

We decided on surgery at a very early stage. However, initially, due to severe swelling around the eye, we refrained from relying on manual measurements of exophthalmos using Hertel exophthalmometry, which tends to be inaccurate in such cases. Instead of manual measurement, the evaluation of the PSI involved comparing bony orbital volume and the degree of exophthalmos before and after surgery. Preoperative data, measured through CT scans immediately after the injury, indicated severe orbital swelling. Typically, patients with orbital wall fractures, excluding blow-in fractures, might anticipate enophthalmos due to increased bony orbital volume. However, immediately after the injury, swelling causes a more significant increase in the intraorbital soft tissue volume than in the bony volume, leading to a tendency for proptosis rather than enophthalmos in the very early stages. Since measurements were taken using CT scans immediately after the injury, the observed tendency was for proptosis rather than enophthalmos, which would be expected after the swelling subsides. Therefore, rather than evaluating the improvement of the degree of enophthalmos, which is typically used in assessing the therapeutic outcomes of orbital fractures, we considered postoperative DVXs as important indicators.

While the bony orbital volume, unrelated to swelling, did not show a statistically significant decrease before and after the operation, the quantitative reduction observed in all cases demonstrated a significant surgical effect. Compared with preoperative measurements, the decrease in exophthalmos after surgery can be attributed to both the reduction in swelling and the surgical effect. In relation to enophthalmos, the cutoff value for DVX measurements is known to be 2 mm.[22] Considering this, the fact that DVX after 6 months of surgery, with improved postinjury swelling, decreased to <1 mm, except in the case of patient 8, indicates a significant surgical effect rather than significant enophthalmos caused by trauma.

Moreover, in the case of patient number 8, although the DVX measurement (1.7 mm) did not reach a sufficiently favorable value after surgery, the DVV after surgery (0.7 mL) improved significantly compared with before surgery. Viewing the success of the operation from a symmetry perspective, the surgical effect was sufficient. The peculiarity in this particular case lies in the degree of exophthalmos on the affected side, which measured 20.8 mm before and 17.2 mm after surgery, a difference of 3.6 mm, larger than that observed in other patients. This suggests that the postinjury swelling of patient 8 was more severe, resulting in greater improvement and raising the possibility of considering soft tissue injury.

Using the independent t test, statistical analysis revealed no significant difference in bony orbital volume and the degree of

exophthalmos on both sides before and after surgery. However, Pearson correlation coefficient test showed increased R-values after surgery, confirming quantitative restoration of postoperative bony orbital volume and degree of exophthalmos using PSI.

This study was limited by its small sample size of only 12 cases due to being conducted as an IND clinical trial, resulting in inadequate statistical power. In addition, as a single-arm study, while there is an excellent benchmark of the opposite eye for comparison, the lack of another treatment as a control group prevents a direct comparison of the superiority of surgical treatment. Furthermore, 2 patients were excluded from follow-up observation; although no adverse effects were confirmed over the phone, the loss to follow-up of 2 out of 12 patients is not insignificant. Therefore, subsequent research should focus on specifying control groups and increasing the number of patients.

CONCLUSIONS

The 3-dimensional PSIs, customized to each patient's unique fracture shape and characterized by 2 separate implants and locking parts with notches, can ensure the restoration of bony orbital volumes and the degree of exophthalmos. Moreover, they have proven feasible and applicable to reconstruct acute orbital wall fractures.

ACKNOWLEDGMENTS

The authors thank Dong Ryul Song and Seon Jeong Kim from CGBio for the efforts in implant design and fabrication.

REFERENCES

1. Shin JW, Lim JS, Yoo G, et al. An analysis of pure blowout fractures and associated ocular symptoms. *J Craniofac Surg* 2013; 24:703–707
2. Gart MS, Gosain AK. Evidence-based medicine: orbital floor fractures. *Plast Reconstr Surg* 2014;134:1345–1355
3. Young SM, Kim YD, Kim SW, et al. Conservatively treated orbital blowout fractures: spontaneous radiologic improvement. *Ophthalmology* 2018;125:938–944
4. Kim Y, Lim JY, Yang GH, et al. 3D-printed PCL/bioglass (BGS-7) composite scaffolds with high toughness and cell-responses for bone tissue regeneration. *J Ind Eng Chem* 2019;79:163–171
5. Shyu VB, Hsu CE, Chen CH, et al. 3D-assisted quantitative assessment of orbital volume using an open-source software platform in a Taiwanese population. *PLOS One* 2015;10:e0119589
6. Kim SP, Lee BY, Lee SJ, et al. A study on orbital volume of Korean people in their 20s or 40s. *Ophthalmic Res* 2012;47: 98–102
7. Du Y, Lu BY, Chen J, et al. Measurement of the orbital soft tissue volume in Chinese adults based on three-dimensional CT reconstruction. *J Ophthalmol* 2019;2019:9721085
8. Gibson RD. Measurement of proptosis (exophthalmos) by computerized tomography. *Australas Radiol* 1984;28:9–11
9. Singh AK, Khanal N, Chaulagain R, et al. Is the pre-shaping of an orbital implant on a patient-specific 3D-printed model advantageous compared to conventional free-hand shaping? A systematic review and meta-analysis. *J Clin Med* 2023;12:3426
10. Foletti JM, Scolozzi P. Severe distortion of an orbital titanium mesh implant after recurrent facial trauma: a potential threat to the orbital contents? *Br J Oral Maxillofac Surg* 2017;55:836–838
11. Scolozzi P. Maxillofacial reconstruction using polyetheretherketone patient-specific implants by "mirroring" computational planning. *Aesthetic Plast Surg* 2012;36:660–665
12. Schön SN, Skalicky N, Sharma N, et al. 3D-printer-assisted patient-specific polymethyl methacrylate cranioplasty: a case series of 16 consecutive patients. *World Neurosurg* 2021;148:e356–e362
13. Wong KC. 3D-printed patient-specific applications in orthopedics. *Orthop Res Rev* 2016;8:57–66
14. Salmi M, Tuomi J, Paloheimo KS, et al. Patient-specific reconstruction with 3D modeling and DMLS additive manufacturing. *Rapid Prototyp J* 2012;18:209–214
15. Chamo D, Msallem B, Sharma N, et al. Accuracy assessment of molded, patient-specific polymethylmethacrylate craniofacial implants compared to their 3D printed originals. *J Clin Med* 2020;9: 832
16. Moiduddin K, Mian SH, Umer U, et al. Design, analysis, and 3D printing of a patient-specific polyetheretherketone implant for the reconstruction of zygomatic deformities. *Polymers (Basel)* 2023;15: 886
17. Arvidson K, Abdallah BM, Applegate LA, et al. Bone regeneration and stem cells. *J Cell Mol Med* 2011;15:718–746
18. Taniguchi N, Fujibayashi S, Takemoto M, et al. Effect of pore size on bone ingrowth into porous titanium implants fabricated by additive manufacturing: an in vivo experiment. *Mater Sci Eng C Mater Biol Appl* 2016;59:690–701
19. Grimm WD, Dannan A, Giesenhagen B, et al. Translational research: palatal-derived ecto-mesenchymal stem cells from human palate: a new hope for alveolar bone and cranio-facial bone reconstruction. *Int J Stem Cells* 2014;7:23–29
20. Ghasemi-Mobarakeh L, Prabhakaran MP, Morshed M, et al. Bio-functionalized PCL nanofibrous scaffolds for nerve tissue engineering. *Mater Sci Eng C* 2010;30:1129–1136
21. Lee JH, Son JM, Akoh CC, et al. Optimized synthesis of 1,3-dioleoyl-2-palmitoylglycerol-rich triacylglycerol via interesterification catalyzed by a lipase from thermomyces lanuginosus. *N Biotechnol* 2010;27:38–45
22. Garcia BG, Ferrer AD. Surgical indications of orbital fractures depending on the size of the fault area determined by computed tomography: a systematic review (in Spanish). *Rev Española Cir Oral Maxilofac* 2016;38:42–48

